

PROOF COVER SHEET

Author(s): Christian Mata,, Paul M. Walker,, Arnau Oliver,, François Brunotte,, Joan Martí, and Alain Lalande

Article title: ProstateAnalyzer: web-based medical application for the management of prostate cancer using multiparametric MR imaging

Article no: TMIF_A_1008488

Enclosures: 1) Query sheet
2) Article proofs

Dear Author,

Please check these proofs carefully. It is the responsibility of the corresponding author to check against the original manuscript and approve or amend these proofs. A second proof is not normally provided. Informa Healthcare cannot be held responsible for uncorrected errors, even if introduced during the composition process. The journal reserves the right to charge for excessive author alterations, or for changes requested after the proofing stage has concluded.

The following queries have arisen during the editing of your manuscript and are marked in the margins of the proofs. Unless advised otherwise, submit all corrections using the CATS online correction form. Once you have added all your corrections, please ensure you press the “Submit All Corrections” button.

Please review the table of contributors below and confirm that the first and last names are structured correctly and that the authors are listed in the correct order of contribution.

Contrib. No.	Prefix	Given name(s)	Surname	Suffix
1		Christian	Mata	
2		Paul M.	Walker	
3		Arnau	Oliver	
4		François	Brunotte	
5		Joan	Martí	
6		Alain	Lalande	

AUTHOR QUERIES

Q1: Please provide the volume number and page range for Ref. [24].

Q2: Please provide the location for Ref. [33].

- Q3: Artwork will only appear in color in the online journal, please ensure the description of Figure 8 will make sense when it is printed in black and white, amending captions and text as necessary.
- Q4: Please confirm the email address of the corresponding author.

ProstateAnalyzer: web-based medical application for the management of prostate cancer using multiparametric MR imaging

Christian Mata,^{1,2} Paul M. Walker,^{2,3} Arnau Oliver,¹
François Brunotte,^{2,3} Joan Martí,¹ and Alain Lalande^{2,3}

¹Department of Computer Architecture and Technology, University of Girona, Girona, Spain,

²Laboratoire Electronique Informatique et Image (Le2I), Université de Bourgogne, Dijon, France, and

³Department of NMR Spectroscopy, University Hospital, Dijon, France

Objectives: In this paper, we present ProstateAnalyzer, a new web-based medical tool for prostate cancer diagnosis. ProstateAnalyzer allows the visualization and analysis of magnetic resonance images (MRI) in a single framework.

Methods: ProstateAnalyzer recovers the data from a PACS server and displays all the associated MRI images in the same framework, usually consisting of 3D T2-weighted imaging for anatomy, dynamic contrast-enhanced MRI for perfusion, diffusion-weighted imaging in the form of an apparent diffusion coefficient (ADC) map and MR Spectroscopy. ProstateAnalyzer allows annotating regions of interest in a sequence and propagates them to the others.

Results: From a representative case, the results using the four visualization platforms are fully detailed, showing the interaction among them. The tool has been implemented as a Java-based applet application to facilitate the portability of the tool to the different computer architectures and software and allowing the possibility to work remotely via the web.

Conclusion: ProstateAnalyzer enables experts to manage prostate cancer patient data set more efficiently. The tool allows delineating annotations by experts and displays all the required information for use in diagnosis. According to the current European Society of Urogenital Radiology guidelines, it also includes the PI-RADS structured reporting scheme.

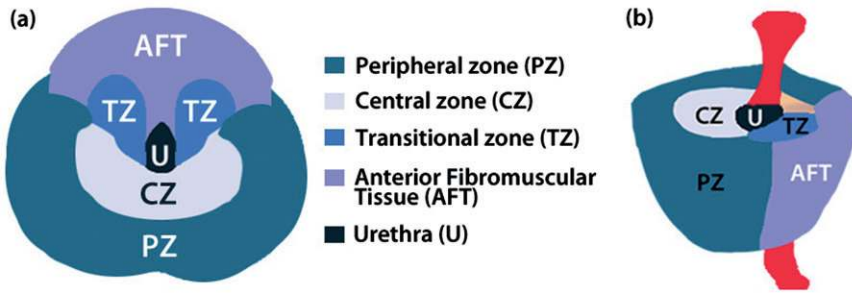
Keywords Applications, database management system, magnetic resonance imaging, magnetic resonance spectroscopy, medical informatics, prostate cancer

BACKGROUND

Prostate cancer (PCa) has become a significant health care burden (1). Early diagnosis and active follow-up allow improved prognosis and prevent life-threatening conditions. Once the decision of treatment is taken, having the most complete set of information for treatment and then for follow up is crucial. Among the techniques used to detect and diagnose PCa, magnetic

Correspondence: Christian Mata, Department of Computer Architecture and Technology, University of Girona, Campus Montilivi, Ed. P-IV, 17071 Girona, Spain. E-mail: cmata@eia.udg.edu

50
 COLOR
 Online /
 B&W in
 Print



59 **Figure 1.** Anatomy of the prostate in (a) transversal and (b) sagittal planes.

62 resonance imaging (MRI) allows the non-invasive analysis of the anatomy and
 63 the metabolism in the entire prostate gland. The prostate is composed of
 64 peripheral (PZ), central (CZ), transition (TZ), and anterior fibromuscular
 65 tissue (AFT) zones (Figure 1). The PZ represents up to 70% of a normal
 66 prostate gland and around 75% of prostate cancers originate in this zone. The
 67 CZ represents about 25% of a normal healthy prostate gland in a young adult.
 68 Even if the frequency of cancers originating here is much lower, they tend to be
 69 of the more aggressive type (2).

70 MRI has been established as the best imaging modality for the detection,
 71 localization, and staging of PCa on account of its high resolution and excellent
 72 spontaneous contrast of soft tissues and the possibilities of multiplanar and
 73 multiparameter scanning (3). As such, three MRI techniques (anatomic 3D
 74 T2-weighted, diffusion-weighted, and perfusion-weighted imaging) and 3D
 75 MR spectroscopy will be illustrated in this paper. A 3D T2-weighted imaging
 76 (T2WI) sequence (4) yields good contrast between PZ and CZ tissues. Diffusion-
 77 weighted imaging (DWI) provides functional information of tissues such as cell
 78 organization, density and microstructure, and depends principally on the
 79 Brownian motion of water molecules (5). It can be displayed either as native
 80 diffusion-weighted images or as the ADC parametric map. The motion of water
 81 molecules is more restricted in tissues with a high cellular density and intact
 82 cell membranes and very low values are clearly indicative of cancer (6).
 83 Perfusion imaging is based on the dynamic contrast enhancement (DCE) of the
 84 signal during the first pass of the contrast agent. The theoretic underpinnings
 85 of this vascular technique are based on tumor angiogenesis. In fact, there is a
 86 relationship between abnormal perfusion and neoangiogenesis in tumors
 87 (7–9). Magnetic resonance spectroscopy (MRS) is a technique that allows the
 88 study of metabolite concentrations by means of a 3D chemical shift imaging
 89 protocol (10). This study is useful since healthy and cancer tissues show
 90 different concentration levels. Specifically, prostate cancer tissues show lower
 91 levels of citrate and higher levels of choline compared with healthy tissue
 92 (11–15) and metabolic data are often presented in the form of concentration
 93 ratios, e.g. [Choline + Creatine]/Citrate. The exact ratio can vary with equip-
 94 ment and settings. For example, ratios at 3 T differ slightly from those at 1.5 T
 95 because of differences in the shape of the citrate spectrum (16). However, it is
 96 generally accepted that PZ zone voxels, in which the ratio of choline and
 97 creatine to citrate is at least two SDs higher than the average ratio in healthy
 98 tissues, are considered to represent possible cancer (17). Voxels are considered

99 highly suggestive of cancer if the ratio of choline and creatine to citrate is more
100 than three SDs higher than the average ratio (18).

101 The increasing amount of data available to analyze a study has not been
102 accompanied with the development of a single standardized way to report it.
103 Often the reports have been unstructured and in a narrative way (19).
104 However, the European Society of Urogenital Radiology (ESUR) has recently
105 proposed the Prostate Imaging-Reporting and Data System (PI-RADS) as the
106 standard structured reporting scheme for prostate cancer (10). Although other
107 schemes exist, such as the Likert score (20), the use of PI-RADS is rapidly
108 extending (21–24). Therefore, we included in our tool the possibility to use this
109 reporting scheme.

110 The medical support systems used to assist the diagnosis of prostate lesions
111 are generally focused on prostate segmentation (25–28). They rely on
112 computerized techniques for prostate cancer detection applied to ultrasound,
113 magnetic resonance, and computed tomodensitometric images (29). For
114 example, Vos et al. (30) used 3D-T2 imaging to define specific regions of
115 interest (ROI), which were subsequently used on diffusion- and perfusion-
116 weighted images to extract relevant features. The purpose was to train and
117 classify the extracted set of features to calculate the likelihood of malignancy.
118 Other related surveys have been focused on magnetic resonance spectroscopic
119 data (31). The rapid growth of computer-based clinical exams has seen a
120 significant increase in the number of online medical imaging systems (32,33),
121 some of which being developed as web-based applications (34). The main
122 challenge is the access and the interaction between the hospital database and
123 the distant users. Thus, the aim of our work was to develop a new architecture
124 system allowing including a web-based application connected to a prostate
125 image database.

126 In the field of biomedical informatics, one of the long standing problems is
127 finding a way to share medical data across a variety of media. Inherently,
128 medical data are generated by a multitude of sources (35,36). eXtensible
129 Markup Language (XML) has emerged as a leading facilitator. Although the
130 XML is provided with predefined tags, one of its advantages is its extensible
131 use. Over the last few years, a set of standards in the medical domain has been
132 developed, called medical markup language (MML) to allow the exchange of
133 medical data between different medical information providers (37,38).
134 Therefore, the XML schema of tags can be defined for each individual case.
135 Finally, the inclusion of the XML databases facilitates the management of
136 XML files by storing them in an efficient way (39). Traditional object relational
137 techniques, based on an XML model, are used to store XML files in an eXist-db
138 database (40).

139

140 **PRIMARY OBJECTIVES**

141
142 In this paper, we propose a new medical tool in the form of an interactive JAVA
143 applet application called Prostate-Analyzer. The purpose is to facilitate the
144 inclusion of medical findings on existing prostate images using the combin-
145 ation of MRI techniques and MR Spectroscopy. The novelty of our proposed
146 framework is that it includes the use of MRI and MRS in a compact
147 application. Generally, users have different tools to evaluate prostate images

148 for MRI and MRS. However, it is necessary to compare regions of interest at
 149 the same time in order to determine pathologies or prostate lesions. For this
 150 reason, it is more efficient for each modality to provide a single tool that can
 151 easily manage all the data.

152 The main objective of the ProstateAnalyzer system is to develop a new tool
 153 that encompasses the visualization and analysis of prostate MR images, as
 154 well as a new storage system of clinical diagnoses in a single package. The tool
 155 is able to characterize the morphological (location, shape, and size) and the
 156 imaging features (mean and standard deviation of the signal, area, and center
 157 of mass) of a region within the image, defined and annotated by an expert.

158 Furthermore, it calculates the signal-time curve in perfusion studies and
 159 displays the LCModel signal spectrum for spectroscopic analysis (41). Besides,
 160 it allows the analysis of the same image by different experts, an essential
 161 feature in order to obtain a robust evaluation. The final outcome of the analysis
 162 is summarized in terms of the PI-RADS protocol.

163 With regard to the proposed architecture for storage of medical images,
 164 this should guarantee the connection and a secured access to the server, the
 165 DICOM database, and the system storage of clinical diagnoses (XML
 166 database).

167

168

169 RESEARCH DESIGN

170

171 Materials

172

173

174

175

176

177

178

179

180

181

182

183

184

185

186

187

188

189

190

191

192

193

194

195 ProstateAnalyzer application

196

197

198 ProstateAnalyzer is a network-based database system whose aims are the man-
 199 agement and processing of both MRI and MRS data sets in a single package.

197
 COLOR
 Online /
 B&W in
 Print

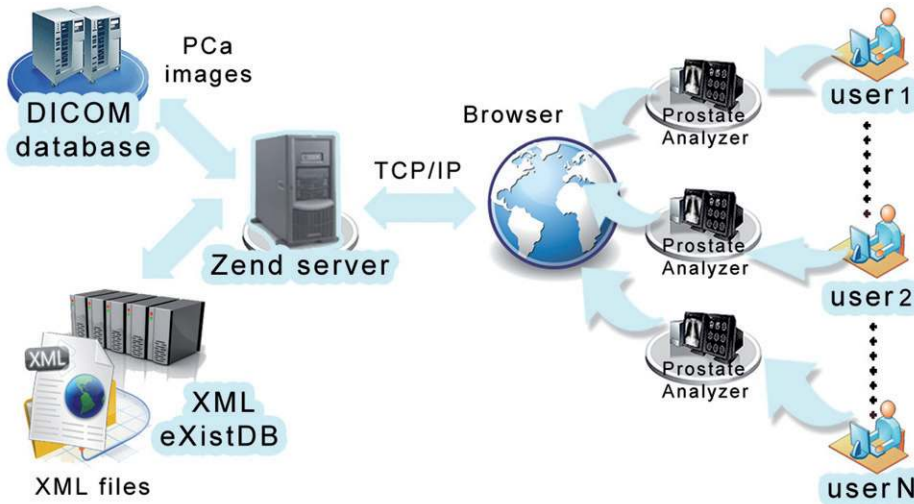


Figure 2. Network-based database system designed to implement the framework and the used hardware. The Zend server allows easy integration of the Apache server with database management tools.

This tool is implemented as a Java-based applet application to facilitate the inclusion of medical findings on existing prostate studies.

Architecture

A system has been designed in order to link the ProstateAnalyzer application to a database of DICOM images and a XML server, which stores the annotated files of the DICOM images. This architecture is supported by a Zend Server in order to allocate the ProstateAnalyzer application and a XML database provided by eXist-db (40). This type of architecture has been used in previous works for supporting other modalities of medical imaging databases such as PACS (42).

The ProstateAnalyzer application (Figure 2) communicates via socket TCP/IP with the Apache Server provided by Zend Server. This server is connected to a DICOM database, containing DICOM prostate images and with the eXist-db database, containing the XML files. We opted for the creation of the XML annotation files in the database in order to preserve the integrity of the original DICOM database (usually stored in a PACS system).

Furthermore, in order to avoid vulnerabilities during the transfer of information, internal security measures have been implemented. Besides using control User ID private keys, the algorithms have systems that protect and encrypt the information during its transmission. Currently, the secure socket layer (SSL) cryptographic protocol is used (43). Finally, the users can download the complete analysis performed by one user in a PDF file such a pre-medical report.

XML database

The ProstateAnalyzer application is related to the eXist-db manager, responsible for the XML database, incorporating its own server for access and management via web interface. We also opted for the creation of the XML

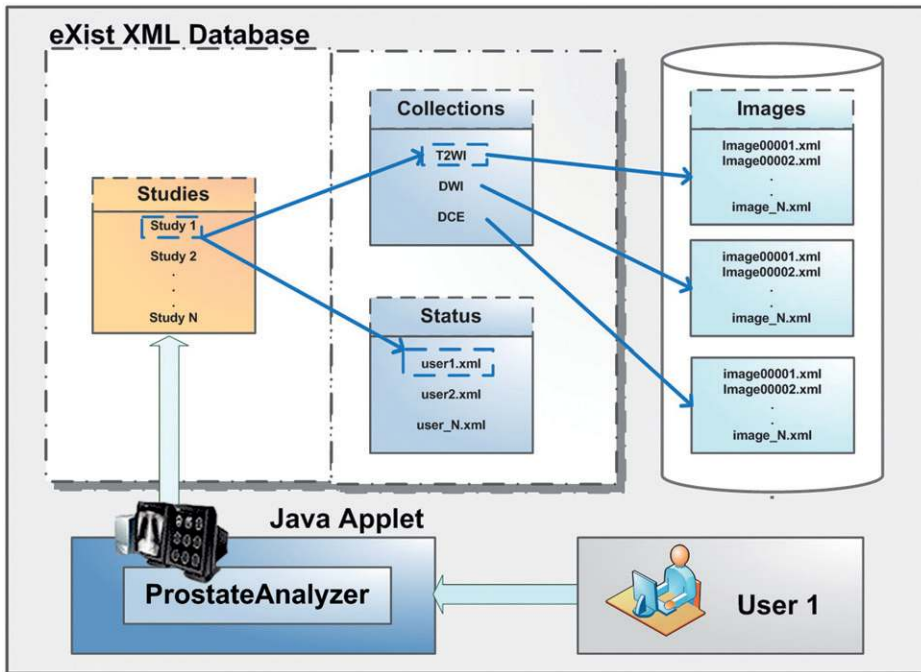


Figure 3. Connections to the eXist XML database within the ProstateAnalyzer and its interaction with the user.

annotation files in the database. Again, all XML files are related to their corresponding DICOM images and contain the records provided by experts.

Figure 3 shows a scenario of the use of the eXist-db XML database. The database is configured at different levels in order to store XML files associated with studies, collections, status and images. First, the ProstateAnalyzer application connects with the eXist-db to access a study, where each study contains a set of XML collections corresponding to 3DT2, DWI (as ADC map), and DCE techniques. Consequently, for each dataset, all the XML files concerning prostate images are allocated. It is important to note that each XML file contains the annotations provided by all the experts. In this way, the main structure of the XML file is the same for the images of the same study, thus enabling a faster access to the annotated information.

Moreover, at the status level, for each study, a XML file associated with each user is saved. Consequently, once the user is logged into the ProstateAnalyzer, the corresponding XML file is obtained.

Security and system access

ProstateAnalyzer is designed as a web application; hence the connection between the applet and the server can be both internal and external. The actual login process consists in an authentication measure with a unique username and password. One of the key elements in this application concerns the security of the data and the information across the network. In this sense, internal security measures to avoid vulnerabilities from the transfer of information are already included in the Zend Server.

HTTP was originally designed for the transmission and reproduction of multimedia documents, but these encodings are not part of the HTTP standard.

295 It is up to the applications themselves to break down and reassemble the
296 information in order to transmit and receive it. Fortunately, Java applets are
297 inherently based on the Internet Inter-ORB Protocol (IIOP). This protocol is
298 based on the client/server computing model and a security algorithm is
299 implemented as a security mechanism to ensure the integrity of the medical
300 data being transferred. In the literature, several architectures use the IIOP
301 in their security applications (19,44).

302 The most widely used regulations with respect to privacy and security are
303 the Health Insurance Portability and Accountability Act (HIPAA) and the
304 European Data Protection Directive 95/46/EC. Both regulations mandate
305 health institutions to protect health information against unauthorized use or
306 disclosure (45). In ProstateAnalyzer, the login/password signature allows
307 knowledge of who is dealing with the individual data. Therefore, an audit-log
308 for each study is produced identifying the user who has read the data and
309 thereby allowing one to generate audit trails on data access activities for any
310 specific patient (46).

311

312 **ProstateAnalyzer engine**

313 The search engine is the front-end for users once ProstateAnalyzer is accessed.
314 There are two types of patient searches: search for all the patients and an
315 advanced search. In the first option, the search engine returns a list with all
316 the patients recorded in the database. In the second case, the system returns
317 just the patients who share the same regular expression used as a query. To
318 perform a search, it is necessary to create a data set that contains information
319 concerning the four MR modalities described before. For each item, the tool
320 shows different attributes (patient name, comments, and status) and the
321 number of images provided by the concerned modality (anatomy, diffusion,
322 perfusion, and spectroscopy). Moreover, each case is represented by a different
323 color depending on the status of the study. When a state is color-coded as
324 yellow, it means that the study has been analyzed partially; a green color-
325 coding indicates that the study has been completely analyzed and validated.
326 Finally, white represents a study that has not yet been analyzed.

327

328 **Anatomy 3D-T2WI**

329 ProstateAnalyzer offers a new visualization platform to provide annotations
330 for different kinds of tissues (tumor number 1, tumor number 2, PZ, CZ, TZ, or
331 others) obtained from T2WI studies. This visualization capability is combined
332 with basic post-processing tasks such as zooming, gamma correction, user-
333 specific ROI, surface, and volumetric measurements. In addition, the viewer
334 provides information from the DICOM header, the status of the anatomical
335 study (validated, partial, or empty) and the list of the annotations added by
336 different users.

337 **Figure 4(a)** shows an example of visualization of the T2WI in prostate
338 cancer analysis. When an overlay is manually drawn, a label is automatically
339 defined with the user's specified color. This label is defined using the first
340 letter of the user's first name and surname followed by the number of
341 annotations (in the figure, the first region of interest is identified by letters
342 "AL0" in green). A table shows a list of color-coded overlays, specifying the
343 username and the tissue type (indicated by the user). It also allows us to

344
345
346
347
348
349
350
351
352
353
354
355
356
357
358
359
360
361
362
363
364
365
366
367
368
369
370
371
372
373
374
375
376
377
378
379
380
381
382
383
384
385
386
387
388
389
390
391
392

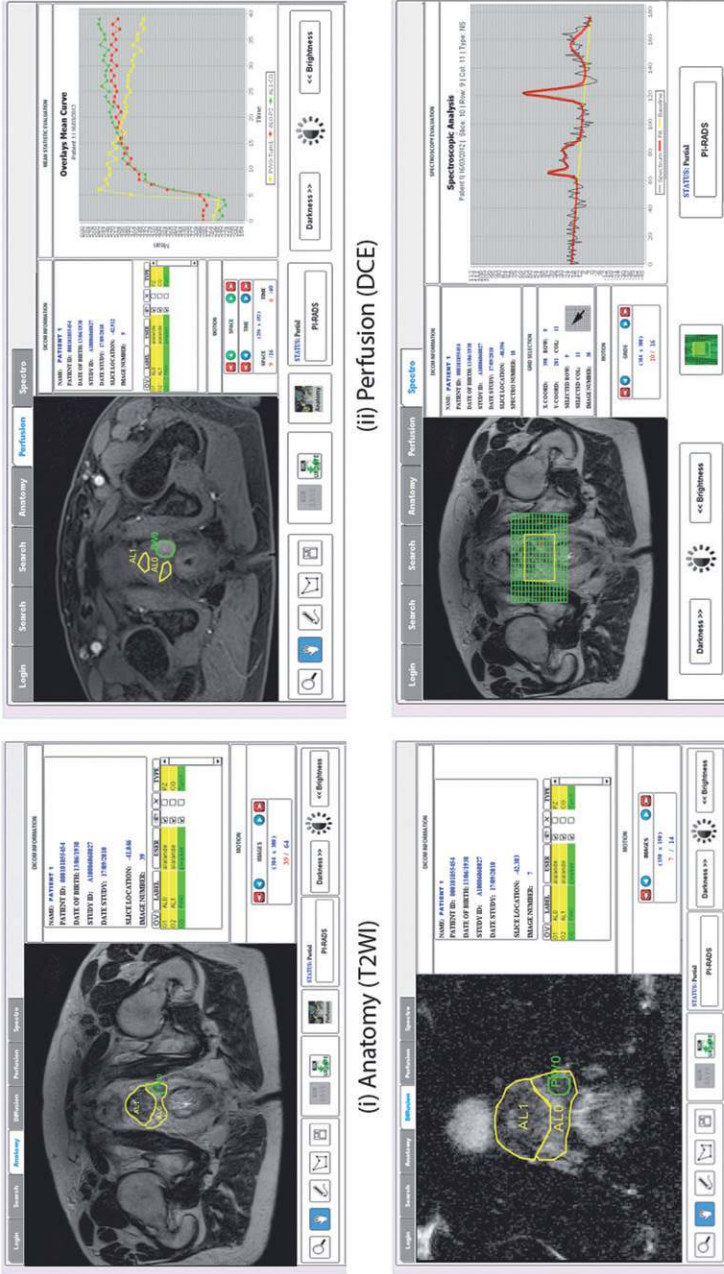


Figure 4. The four visualization screens of ProstateAnalyzer. Notice that all of them follow the same structure, with the corresponding image in the left part, the information of the image or related with the specific modality in the right part, and the imaging tools in the bottom part of the image. (a) T2WI, (b) DWI, (c) DCE with corresponding signal-time curves, and (d) MRS with a LCModel-processed signal spectrum.

visualize or to delete each overlay, although this latter option is only available to the expert who created it. Selecting an overlay of the table allows displaying its related information (the annotations filled in a pop-up window). Finally, after pressing the confirmation button of the pop-up window, the overlay is added to the table, displayed on the image and stored in the XML database.

DWI

ProstateAnalyzer also provides a support tool for the DWI studies with similar basic post-processing tasks as presented previously for T2WI. [Figure 4\(b\)](#) shows an example of an ADC map with annotations provided by different users. In the example, a multiple user-specific region of interest (ROI) study is presented.

Perfusion imaging analysis (DCE)

Dynamic contrast enhanced (DCE) MRI is also catered for in the ProstateAnalyzer. The tool also contains basic post-processing tasks using the same features applied in T2WI and DWI. The most important difference with respect to the other techniques is that the perfusion images are displayed in time-space partitions.

Furthermore, this viewer uses a mean signal-time curve to display the signal enhancement during the arrival of the contrast agent into the tissue. [Figure 4\(c\)](#) shows an example of the ROI analysis in perfusion MR images. For each overlay, the mean signal from each ROI is calculated and displayed as the corresponding signal-time curve: the mean-curve is denoted with a different color according to its associated area.

MRS

ProstateAnalyzer offers individual spectrum visualization from a 3D spectroscopic grid. [Figure 4\(d\)](#) presents an example of a MRS study with a LC Model-processed signal spectrum. This viewer displays a set of 3D-T2 images allowing the spatial location of the spectroscopy study. For each spectroscopic grid, there is a corresponding image. In order to obtain a specific spectrum, the user must click on the corresponding voxel (highlighted in red) within the grid. The LC model is widely used for processing clinical single and multi-voxel spectroscopic data (47). It allows individual and batch analyses of the main metabolites within the spectra of the prostate: citrate, choline, creatine, and spermine.

Interaction between spectroscopy and anatomy

One of the most important features of ProstateAnalyzer is the interaction of the imaging modalities among themselves. [Figure 5](#) shows an example of the interaction between MRS and T2WI. The aim is to display the annotations, obtained from the T2WI study panel, on the spectrum illustrated within the graphical window. The way to link the processing is provided by the slice location (it is shown in the DICOM information panel of the MRS image, and boarded in yellow). In the MRS study panel, when the expert selects a voxel within the spectroscopic grid, the spectrum is displayed. The next step is to determine whether the selected voxel contains any annotations from the anatomical 3D-T2 panel. If the information exists, it is displayed in the

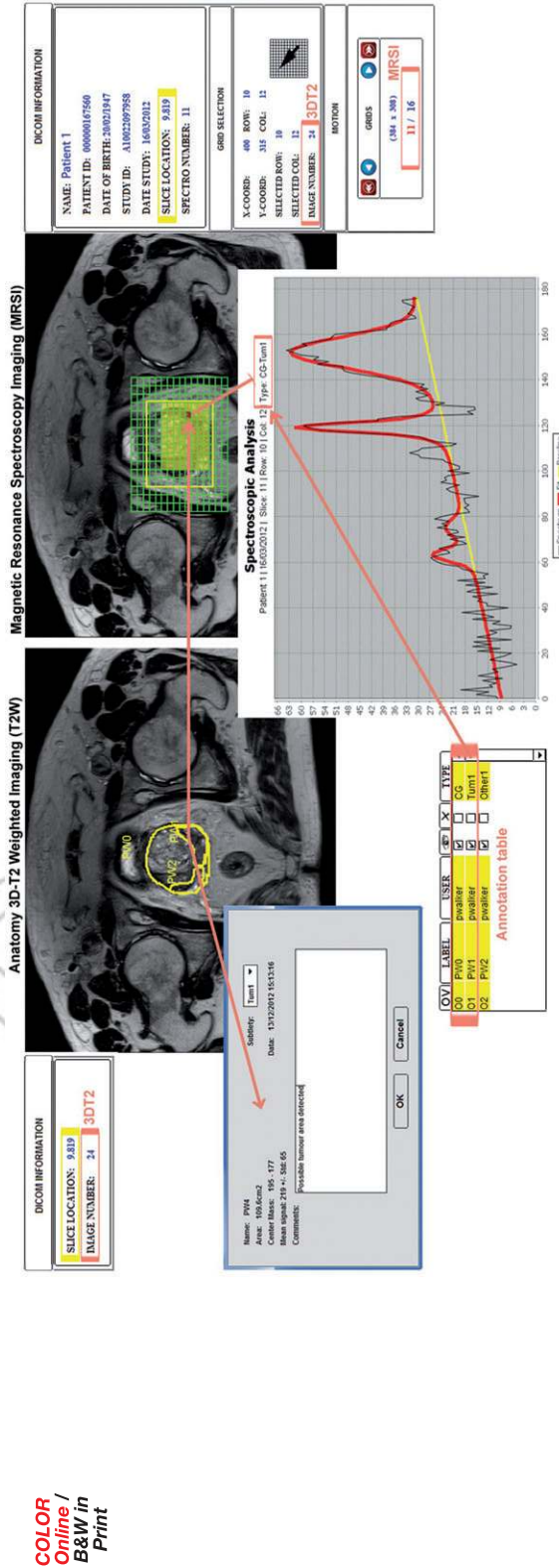


Figure 5. Example of the interaction between a 3D spectroscopic imaging study with T2W imaging.

491 spectroscopic graphical area along with the spectrum. The example shows the
492 selected voxel corresponding to an area (in the anatomic analysis) with two
493 denominations for one tissue (named as Tum1 and CG in the figure), and is
494 also represented on the annotation table. This interaction is very important,
495 because one can visualize the information of both techniques in only one
496 representation.

497

Interaction between anatomy and perfusion

498

499

500

501

502

503

504

505

506

507

508

509

510

511

512

513

514

515

516

517

518

519

520

521

522

523

524

525

526

527

528

529

In this case, the anatomic and perfusion studies are not using the same reference image due to the differences in spatial resolution. Consequently, the solution is to locate the image from a set of corresponding perfusion DCE-MRI images, as close as possible, to the slice location of the anatomical 3D-T2 image.

Figure 6 shows an example of the analysis on a perfusion-weighted study using the ROI drawn on the corresponding 3D-T2 image. On the interface of the perfusion image analysis, when the “anatomy” button is pressed all the annotations concerning the anatomy study are displayed. ProstateAnalyzer adapts the annotated regions into the correct position in the perfusion image, according to the spatial resolution and the pixel spacing. In order to distinguish the overlays between perfusion and anatomy, the viewer displays all the anatomy overlays and adds the prefix “A” before the label name.

Reporting

Once the study is analyzed, the findings need to be reported, if possible in a standardized way. ProstateAnalyzer includes the PI-RADS structured reporting scheme, according to ESUR prostate MR guidelines in 2012 (10), which is being established as the common protocol in European countries (21,22). The use of a standardized graphic reporting scheme facilitates the communication with referring colleagues, and it increases the quality and diagnostic value of prostate analyses.

The inclusion of the PI-RADS is carried out using a form with a drop-down list that includes the different answers of the PI-RADS question. Selecting the option, the corresponding number is assigned. The report is saved in an independent XML file and loaded into the XML database. The use of an independent XML file allows a faster search when looking just for similar cases in terms of PI-RADS scores. Besides, there is the option of downloading a PDF file with that information.

527

528

529

MAIN OUTCOME

530

531

532

533

534

535

536

537

538

539

In this section, a complete example of use of the ProstateAnalyzer application is presented. In order to display the environment of the application, the obtained results using the four visualizations platform (T2WI, DCE, DWI, and MRS) are fully detailed. The main purpose is to demonstrate the usability of the ProstateAnalyzer application in the localization and the analysis of a tumor, if present.

Clinical diagnosis

The upper image of Figure 7 shows an example of a localized tumor displayed on T2WI. Prostate cancer usually shows low signal intensity on T2WI that is

540
541
542
543
544
545
546
547
548
549
550
551
552
553
554
555
556
557
558
559
560
561
562
563
564
565
566
567
568
569
570
571
572
573
574
575
576
577
578
579
580
581
582
583
584
585
586
587
588

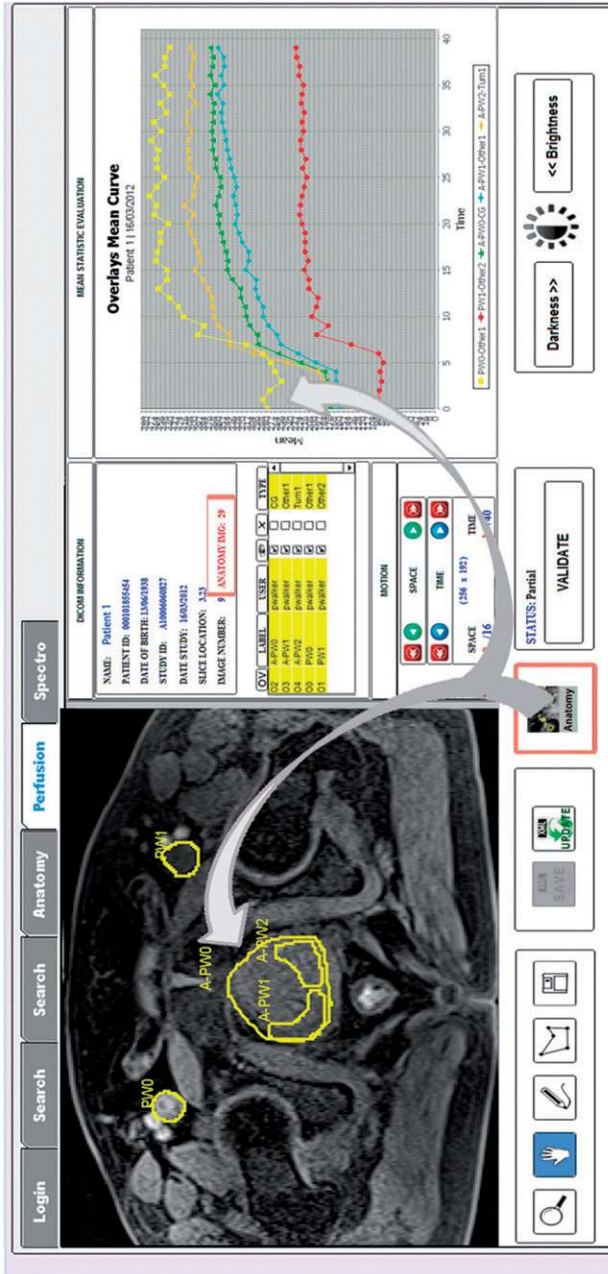


Figure 6. Example of the interaction between a perfusion slice with a 3DT2 image.

589
 COLOR
 Online /
 B&W in
 Print

592
 593
 594
 595
 596
 597
 598
 599
 600
 601
 602
 603
 604
 605
 606
 607
 608
 609
 610
 611
 612
 613
 614
 615

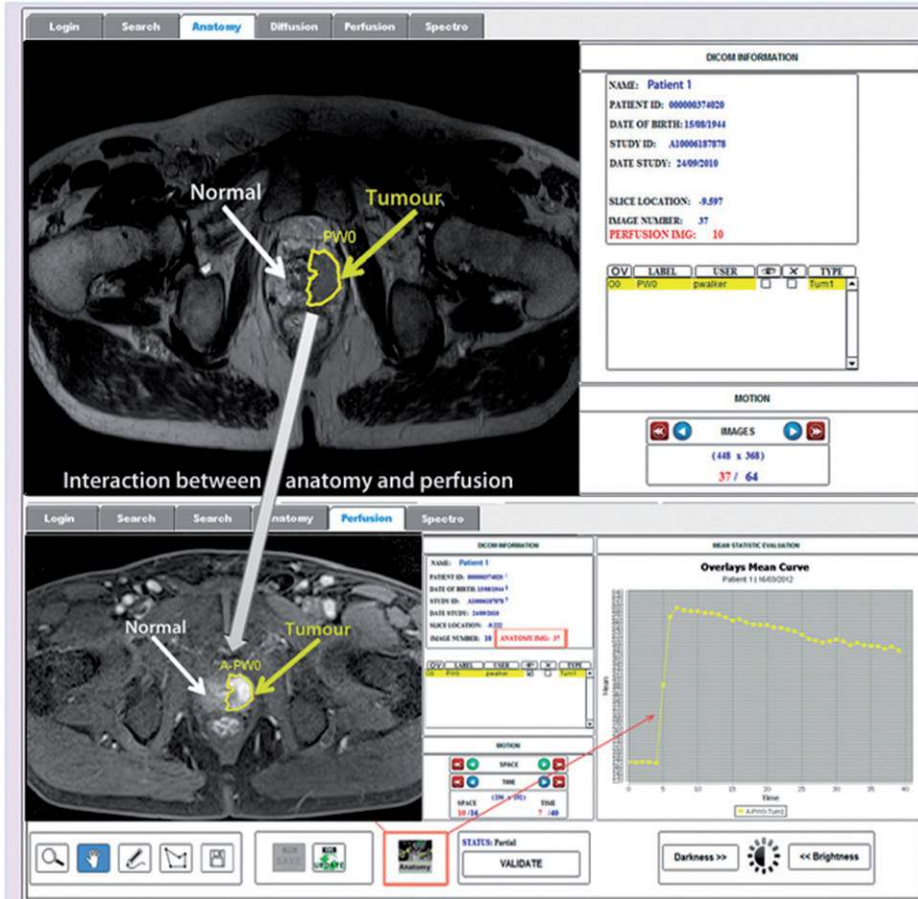


Figure 7. Interaction between T2WI and DCE.

616
 617
 618
 619
 620
 621
 622
 623
 624
 625
 626
 627
 628
 629
 630
 631
 632
 633
 634
 635

well defined with respect to normal PZ zone tissue. However, it is not always easy to localize a pathologic area. One of the advantages of the ProstateAnalyzer application is to analyze the same study using other techniques. Once a sequence of the T2WI is analyzed, the application offers an efficient solution to compare the same ROI in DCE, DWI, and MRS. On the DCE, the peak of the curve corresponds to the first pass of the contrast agent and indicates the rapid uptake of the contrast agent, typically observed in cancer tissue.

We compare the mean curve of a representative tumor tissue with that of healthy tissue in Figure 8. The first curve (in yellow) is from tumor tissue and the second from healthy tissue (in red). In this case, the first annotation corresponds to a tumor region labeled as “PW0” which is made in the perfusion panel. The second, which represents healthy tissue, is annotated in the anatomical panel and displayed in the perfusion panel labeled as “A-PW0”. In the diffusion panel, the analysis also demonstrates the presence of a tumor (Figure 9). It is important to notice that the user draw a different ROI as the one in Figure 7. Indeed, the tumor will correspond to low signal (therefore, low diffusion coefficient) on the ACD map.

636
 637

On the MRS panel (Figure 10), the example shows a selected voxel corresponding to an area of cancer tissue (Tum1). The LC Model-processed

638
639
640
641
642
643
644
645
646
647
648
649
650
651
652
653
654
655
656
657
658
659
660
661
662
663
664
665
666
667
668
669
670
671
672
673
674
675
676
677
678
679
680
681
682
683
684
685
686

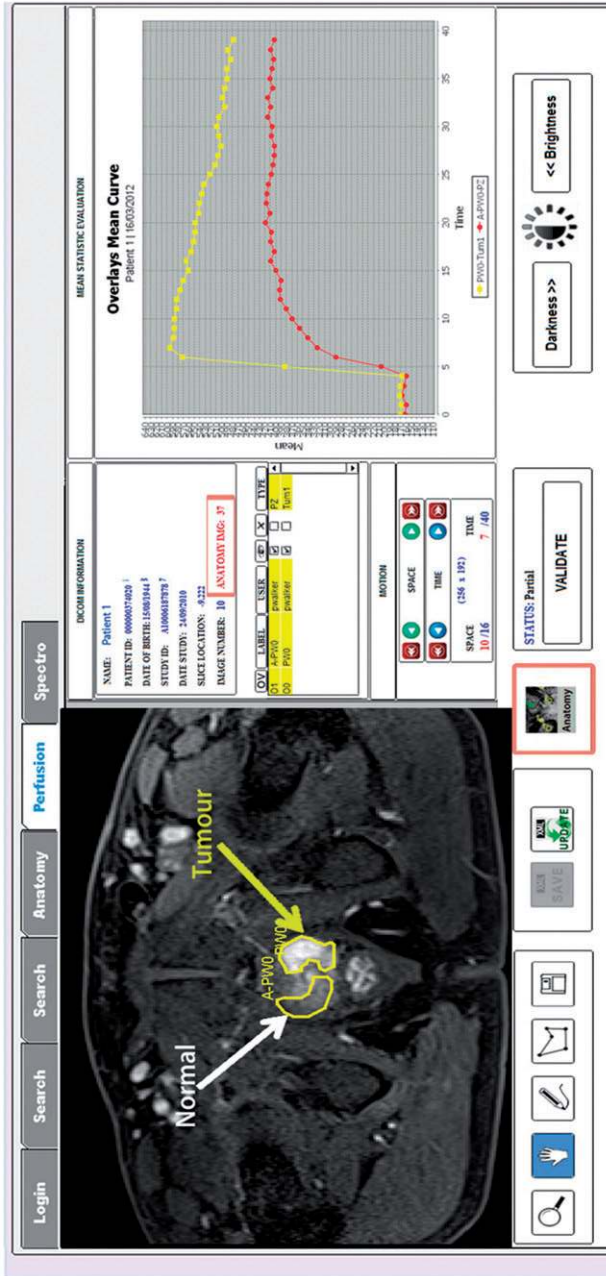
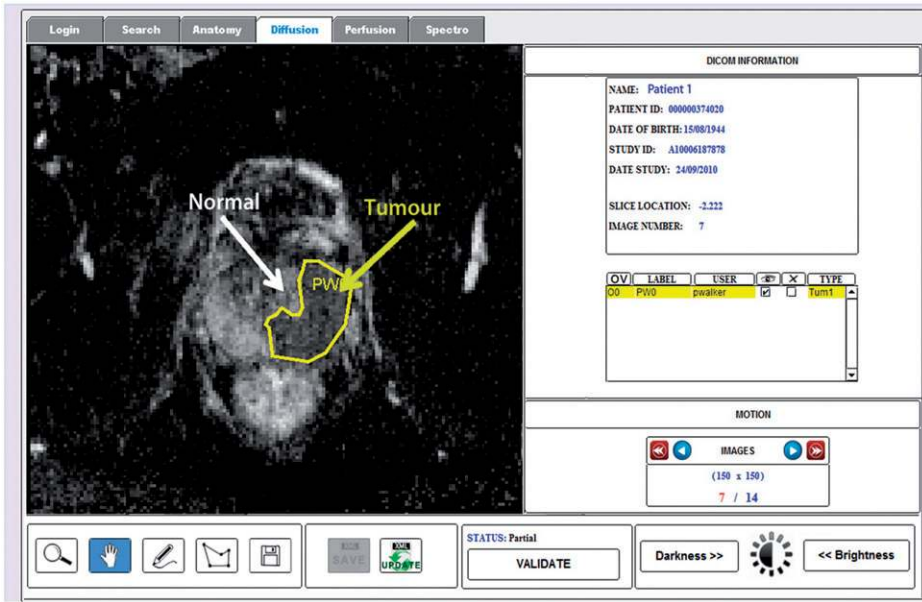


Figure 8. Example of two annotated regions (tumor and healthy) represented in perfusion analysis. A schematic illustration of time-mean curve for DCE is also depicted in both cases (tumor in yellow, healthy area in red).



687
 COLOR
 Online /
 B&W in
 Print

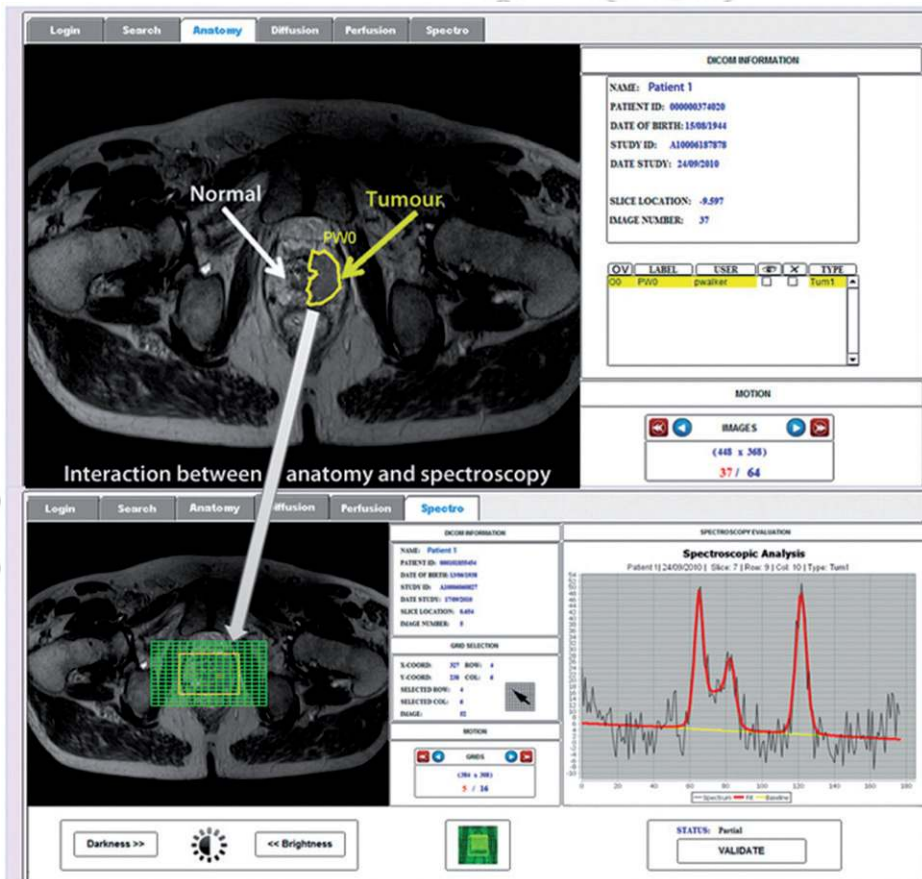
690
 691
 692
 693
 694
 695
 696
 697
 698
 699
 700
 701
 702
 703
 704



705 **Figure 9.** Example of a localized tumor is represented using diffusion-weighted imaging
 706 of the same prostate study.

708
 COLOR
 Online /
 B&W in
 Print

711
 712
 713
 714
 715
 716
 717
 718
 719
 720
 721
 722
 723
 724
 725
 726
 727
 728
 729
 730
 731
 732
 733



734 **Figure 10.** Example of the interaction between T2WI and MRS studies showing the
 735 spectra of the cancer Voxel.

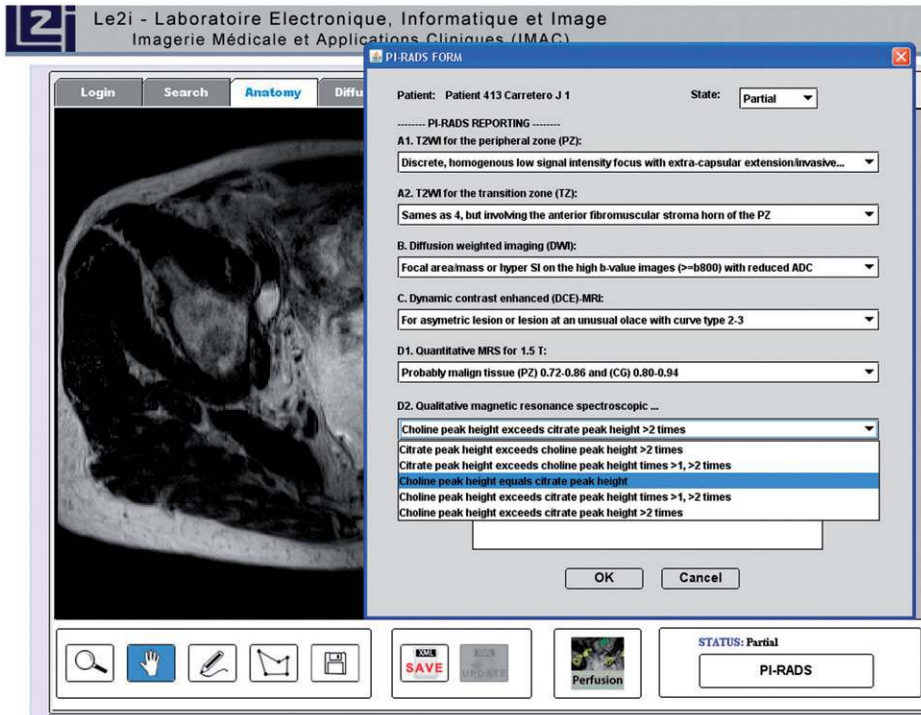


Figure 11. A window pop-up allows to report the case according to the PI-RADS protocol.

signal spectrum demonstrates how the signal is modeled in red from the noisy signal in black. Hence the different peaks of the spectrum are easily extractable. Illustrating graphically the levels of these metabolites is very important, since cancerous tissue is characterized within the spectrum as reduced citrate and elevated choline peaks. In the figure, the first two consecutive peaks correspond to choline and creatine, while the third one corresponds to citrate. It is clear that the relative levels of choline and creatine are very different to those observed in normal healthy tissue (Figure 4d), where higher levels of citrate and lower levels choline are observed.

Once the clinical diagnosis has been performed, users have the option to create a MR reporting, as depicted in Figure 11. For each MR technique, a “PI-RADS” button is available in the option panel. When it is pressed, a window pop-up appears where the user can report the findings for each technique according to the PI-RADS protocol.

Design effort benchmarks

ProstateAnalyzer is currently being used in the MR department of the University Hospital of Dijon (France). The present working database is composed of more than 1600 patient datasets. The time to access to the Java Applet application (ProstateAnalyzer) by users is around 2–3 s in an intranet environment. It has been tested with the following common internet web browsers: Mozilla Firefox, Internet Explorer, Google Chrome, and Opera. It is preferable to use the Java Deployment Toolkit 6.0.160.1.1 or superior and to use the JavaTMPlatform SE 6 U16 6.0.160.1. The most time-consuming part corresponds to loading a prostate study. A typical study consists of a set of

785 64 anatomical images, 14 ADC images, 640 perfusion images, and a set of
786 spectroscopic data containing up to 1000 files. It is important to note that the
787 number of spectroscopic data files is very variable and depends on the prostate
788 size. The average of the time consuming is around 60–70 s to load and display
789 a typical prostate study with the data presented previously.

790 The search engine provided by ProstateAnalyzer is tested in order to obtain
791 the complete study. The timing response to retrieve a prostate study was
792 around 1 min including the corresponding XML-associated files. The time
793 necessary to record annotations on the database is around 3–5 s for anatomical
794 and diffusion images and around 12 s for perfusion images. The computational
795 cost is higher for the latter because of the need to calculate the signal-time
796 curve. In order to obtain a spectrum, the cost is around 5 s to display it in the
797 graphical window. Once the analysis is finished by the user, ProstateAnalyzer
798 takes around 4 s to save the XML file into the database.

799 With the new architecture, ProstateAnalyzer can also be accessed using
800 regular external network connections outside the intranet connection of the
801 hospital. We tested the connection from Girona in Spain (several hundreds of
802 kilometers from Dijon). Experiments were carried out by loading a large study
803 consisting of a set of 64 anatomical images, 15 ADC images, 720 perfusion
804 images, and a set of spectroscopic data containing up to 1200 files (corres-
805 ponding to around 150 MB of transferred data). We loaded the case several
806 times during a week, and the total elapsed time response varied between 100
807 and 130 s. When comparing the times provided by the internal and external
808 connections using the same study, the difference was found to be around
809 40–70 s. The difference was due to two main reasons. On one hand, it depends
810 on the instantaneous network load and on the other hand to the number of
811 users being connected to the ProstateAnalyzer server. The main conflict, when
812 multiple users are connected, is in the downloading of the cases, since the
813 server must split the downloading process between the connected users.
814 However, once the study is loaded, the usability, visualization, and annotation
815 times are independent with respect to the number of users – they just depend
816 on their own machine, not on the server).

817 818 **DISCUSSION** 819

820 ProstateAnalyzer is a web-based application for the analysis of prostate
821 images using four MR modalities: T2WI, DWI, DCE, and MRS. One of the
822 most evident advantages of ProstateAnalyzer is that it allows simultaneous
823 analysis of a prostate study using the different modalities. It also provides an
824 interaction among them and MR spectroscopy. Since the application has been
825 designed to work with DICOM files, any equipment that operates under such
826 image standard can potentially be used with ProstateAnalyzer.

827 The principal problem encountered in the diagnosis of a prostate study is
828 the localization of a ROI-containing tumor tissue. Normally, experts use
829 different tools to validate the diagnoses using different software and make
830 many annotations in different files. This is not a practical solution to managing
831 abundant medical data. ProstateAnalyzer offers the solution, because it allows
832 experts to analyze prostate ROI on T2WI, DWI, DCE, and MRS panels within
833 the same application.

834 The development of the proposed interface has been made in such a way
835 that it is simple and intuitive to use for the users. The interface is divided in
836 four panels with the purpose of visualizing a patient study, simultaneously, for
837 the different techniques. The main objective was to provide useful tools for
838 experts to manage examinations with different types of images and data.
839 ProstateAnalyzer allows the annotation of findings provided by different
840 experts in the prostate. All annotations are saved in XML files associated with
841 the prostate images. Although a prostate study can be shared among all the
842 users, they can still validate or modify their own diagnosis in individual cases.

843 Finally, our tool offers the possibility to work remotely via the web and
844 represents an improvement in the data management. The access to the
845 ProstateAnalyzer should be provided to multiple users in order to make easier
846 both local and external connections. In order to facilitate this task, the
847 application is implemented as a JAVA applet tool. Thus, it is not necessary to
848 install any program on computers to run our interface unless users have a
849 browser that supports Java technology. Moreover, applets can be executed
850 from any operating system (Windows, Linux, and MAC) because they are
851 running in a Web browser. ProstateAnalyzer can be integrated in a server to
852 manage medical images stored in a prostate database.

853 ProstateAnalyzer still presents some limitations which will be addressed in
854 order to enrich the tool. For instance, in perfusion analysis, the tool uses a
855 mean DCE signal–time curve to display the signal enhancement during the
856 arrival of the contrast agent into the tissue. However, providing quantitative
857 values related to microvascular permeability, K^{trans} or the diffusion space, v_e
858 could also be helpful. With regard to the spectroscopy section, the possibility of
859 displaying 2D and 3D metabolite maps will be addressed. For this task,
860 specialized spatial and spectral data processing methods, for which sources are
861 not commonly available, are needed (e.g. morphological analysis and spectral
862 characteristics of the observed metabolites). We are also trying to improve the
863 efficiency of the computational cost. One solution could be to load single frames
864 only, on the basis of their spatial correspondence, instead of the whole dataset.
865 This would also allow the possibility of automatically displaying the four
866 sequences simultaneously. Thus, when scrolling the slices, the information
867 will change simultaneously on the T2WI, DWI, DCE, and MRSI displays.

868 Taking into account how rapidly clinical databases are growing,
869 ProstateAnalyzer should be an important contribution to the management of
870 large databases. Indeed, the implementation of ProstateAnalyzer offers the
871 possibility to extend and adapt to other MR modalities. As a proof of concept,
872 this project is an adaptation from previous work based on mammography (42)
873 and it demonstrates that our approach is easily portable to other sources of
874 medical images. Finally, as ProstateAnalyzer allows downloading reports in
875 PDF format containing the annotations and graphical results (mean signal–
876 time curve and signal spectra), it should also be useful as a pre-report.

877

878

879

CONCLUSION

880 In this paper, we have presented ProstateAnalyzer, a new medical tool
881 that allows the evaluation of the prostate cancer in an effective
882 way. ProstateAnalyzer visualizes the different MRI techniques

(anatomy, diffusion, and perfusion) together with MR spectroscopy, and automatically places annotations, made in one of the images, onto the others. In addition, ProstateAnalyzer also includes the PI-RADS reporting protocol, thereby offering the possibility to fully report the prostate study in a standardized way.

It has been implemented as an interactive JAVA applet application with the purpose of facilitating the inclusion of medical findings on existing prostate images, using the combination of MRI techniques and MR spectroscopic analysis. Furthermore, a new architecture is presented to store the medical records in a XML database which stores a set of annotated files.

DECLARATION OF INTEREST

The authors report that they have no conflicts of interest. This work was partially funded by the Spanish R+D+I Grant no. TIN2012-37171-C02-01. C. Mata holds a Mediterranean Office for Youth mobility grant. Finally, the Regional Council of Burgundy under the PARI 1 scheme sponsored this work.

REFERENCES

1. Schröder FH, Hugosson J, Roobol MJ, et al. Prostate-cancer mortality at 11 years of follow-up. *N Engl J Med* 2012;366:981–90.
2. Verma S, Rajesh A. A clinically relevant approach to imaging prostate cancer: review. *Am J Roentgenol* 2011;196:S1–10.
3. Chen M, Dang HD, Wang JY, et al. Prostate cancer detection: comparison of T2-weighted imaging, diffusion-weighted imaging, proton magnetic resonance spectroscopic imaging, and the three techniques combined. *Acta Radiol* 2008;49:602–10.
4. Bitar R, Leung G, Perng R, et al. MR Pulse sequences: what every radiologist wants to know but is afraid to ask. *RadioGraphics* 2006;26:513–37.
5. Kiliçkesmez O, Cimilli T, Inci E, et al. Diffusion-weighted MRI of urinary bladder and prostate cancers. *Diagn Interv Radiol* 2009;15:104–10.
6. Ren J, Huan Y, Wang H, et al. Diffusion-weighted imaging in normal prostate and differential diagnosis of prostate diseases. *Abdom Imaging* 2008;33:724–8.
7. Jackson AS, Reinsberg SA, Sohaib SA, et al. Dynamic contrast-enhanced MRI for prostate cancer localization. *Br J Radiol* 2009;82:148–56.
8. Bard RL. Dynamic contrast-enhanced mri atlas of prostate cancer. New Haven: Springer; 2009.
9. Alonzi R, Padhani A, Allen C. Dynamic contrast enhanced MRI in prostate cancer. *Eur J Radiol* 2007;63:335–50.
10. Barentsz JO, Richenberg J, Clements R, et al; European Society of Urogenital Radiology. ESUR prostate MR guidelines 2012. *Eur Radiol* 2012;22:746–57.
11. Villeirs GM, Oosterlinck W, Vanherreweghe E, De Meerleer GO. A qualitative approach to combined magnetic resonance imaging and spectroscopy in the diagnosis of prostate cancer. *Eur J Radiol* 2010;73:352–6.
12. Créhange G, Parfait S, Liegard M, et al. Tumor volume and metabolism of prostate cancer determined by proton magnetic resonance spectroscopic imaging at 3T without endorectal coil reveal potential clinical implications in the context of radiation oncology. *Int J Radiat Oncol Biol Phys* 2011;80:1087–94.
13. Créhange G, Maingon P, Gauthier M, et al. Early choline levels from 3-tesla MR spectroscopy after exclusive radiation therapy in patients with clinically localized prostate cancer are predictive of plasmatic levels of PSA at 1 year. *Int J Radiat Oncol Biol Phys* 2011;81:407–13.

- 932 14. Parfait S, Walker PM, Créhange G, et al. Classification of prostate magnetic
933 resonance spectra using support vector machine. *Biomed Signal Process Control*
934 2012;7:499–508.
- 935 15. Testa C, Schiavina R, Lodi R, et al. Prostate cancer: sextant localization with
936 MR imaging, MR spectroscopy, and 11 C-choline PET/CT. *Radiology* 2007;244:
937 797–806.
- 938 16. Scheenen TW, Heijmink SW, Roell SA, et al. Three-dimensional proton MR
939 spectroscopy of human prostate at 3 T without endorectal coil: feasibility. *Radiology*
940 2007;245:507–16.
- 941 17. Verma S, Rajesh A, Fütterer JJ, et al. Prostate MRI and 3D MR Spectroscopy: How
942 We Do It. *Am J Roentgenol* 2010;194:1414–26.
- 943 18. Jung JA, Coakley FV, Vigneron DB, et al. Prostate depiction at endorectal MR
944 spectroscopic imaging: investigation of a standardized evaluation system.
945 *Radiology* 2004;233:701–8.
- 946 19. Dickinson L, Ahmed HU, Allen C, et al. Scoring systems used for the interpretation
947 and reporting of multiparametric MRI for prostate cancer detection, localization,
948 and characterization: could standardization lead to improved utilization of imaging
949 within the diagnostic pathway? *J Magn Reson Imaging* 2013;37:48–58.
- 950 20. Villers A, Puech P, Mouton D, et al. Dynamic contrast enhanced, pelvic phased
951 array magnetic resonance imaging of localized prostate cancer for predicting tumor
952 volume: correlation with radical prostatectomy findings. *J Urol* 2006;176:2432–7.
- 953 21. Portalez D, Mozer P, Cornud F, et al. Validation of the European Society of
954 Urogenital Radiology scoring system for prostate cancer diagnosis on multi-
955 parametric magnetic resonance imaging in a cohort of repeat biopsy patients. *Eur*
956 *Urol* 2012;62:986–96.
- 957 22. Rosenkrantz AB, Kim S, Lim R, et al. Prostate cancer localization using
958 multiparametric MR imaging: comparison of Prostate Imaging Reporting and
959 Data System (PI-RADS) and Likert scales. *Radiology* 2013;269:482–92.
- 960 23. Roethke MC, Kuru TH, Schultze S, et al. Evaluation of the ESUR PI-RADS scoring
961 system for multiparametric MRI of the prostate with targeted MR/TRUS fusion-
962 guided biopsy at 3.0 Tesla. *Eur Radiol* 2014;24:344–52.
- 963 24. Reisæter LA, Fütterer JJ, Halvorsen OJ, et al. 1.5-T multiparametric MRI using
964 PI-RADS: a region by region analysis to localize the index-tumor of prostate cancer
965 in patients undergoing prostatectomy. *Acta Radiol* 2014..
- 966 25. Shah V, Turkbey B, Mani H, et al. Decision support system for localizing prostate
967 cancer based on multiparametric magnetic resonance imaging. *Med Phys* 2012;39:
968 4093–103.
- 969 26. Dickinson L, Ahmed HU, Allen C, et al. Magnetic resonance imaging for the
970 detection, localisation, and characterisation of prostate cancer: recommendations
971 from a European consensus meeting. *Eur Urol* 2011;59:477–494.
- 972 27. Fradet V, Kurhanewicz J, Cowan JE, et al. Prostate cancer managed with active
973 surveillance: role of anatomic MR imaging and MR spectroscopic imaging.
974 *Radiology* 2010;256:176–83.
- 975 28. Ghose S, Oliver A, Mitra J, et al. A supervised learning framework of statistical
976 shape and probability priors for automatic prostate segmentation in ultrasound
977 images. *Med Image Anal* 2013;17:587–600.
- 978 29. Ghose S, Oliver A, Martí R, et al. A survey of prostate segmentation methodologies
979 in ultrasound, magnetic resonance and computed tomography images. *Comput*
980 *Methods Prog Biomed* 2012;108:262–87.
- 981 30. Vos PC, Hambroek T, Barenstz JO, Huisman HJ. Computer-assisted analysis of
982 peripheral zone prostate lesions using T2-weighted and dynamic contrast enhanced
983 T1-weighted MRI. *Phys Med Biol* 2010;55:1719–34.
- 984 31. Carroll PR, Coakley FV, Kurhanewicz J. Magnetic resonance imaging and
985 spectroscopy of prostate cancer. *Rev Urol* 2006;8:S4–10.
- 986 32. Oppelt A. Systems for medical diagnostics: fundamentals, technical solutions and
987 applications for systems applying ionizing radiation, nuclear magnetic resonance
988 and ultrasound. Germany: Publicis Publishing; 2005.

- 981 33. Madabhushi A, Dowling J, Huisman H, Barratt D, eds. Prostate cancer imaging.
982 Image analysis and image-guided interventions. Lecture notes in computer science;
983 2011.
- 984 34. Kurc T, Janies DA, Johnson AD, et al. An XML-based system for synthesis of data
985 from disparate databases. *J Am Med Inform Assoc* 2006;13:289–301.
- 986 35. Marcos E, Acuña CJ, Vela B, et al. A database for medical image management.
987 *Comput Methods Prog Biomed* 2007;86:255–69.
- 988 36. Tahmoush D, Samet H. A new database for medical images and information.
989 In: *Proceedings of SPIE – medical imaging 2007: image processing 2007*,
990 San Diego, CA.
- 991 37. Guo J, Araki K, Takada K, et al. The latest MML (Medical Markup Language)
992 version 2.3–XML-based standard for medical data exchange/storage. *J Med Syst*
993 2003;27:357–66.
- 994 38. Guo J, Takada A, Tanaka K, et al. The development of MML (Medical Markup
995 Language) version 3.0 as a medical document exchange format for HL7 messages.
996 *J Med Syst* 2004;28:523–33.
- 997 39. Lindsay, J. XML databases and biomedical informatics. Connecticut: University of
998 Connecticut; 2008.
- 999 40. Meier W. eXist: an open source native XML database in web, web-services, and
1000 database systems. Germany: Springer; 2002:169–83.
- 1001 41. Provencher SW. Estimation of metabolite concentrations from localized in vivo
1002 proton NMR spectra. *Magn Reson Med* 1993;30:672–9.
- 1003 42. Mata C, Oliver A, Torrent A, Martí J. MammoApplet: an interactive Java applet
1004 tool for manual annotation in medical imaging. In: *IEEE international conference*
1005 *on bioinformatics and bioengineering*, 2012, Larnaca, Cyprus: 34–9.
- 1006 43. Sumathi S, Sivanandam SN. Introduction to data mining and its applications; 29 of
1007 studies in computational intelligence. Germany: Springer; 2006.
- 1008 44. Papadakis I, Chrissikopoulos V, Polemi D. Secure medical digital libraries. *Int J*
1009 *Med Inform* 2001;64:1–8.
- 1010 45. Zhou Z, Liu BJ. HIPAA compliant auditing system for medical images. *Comput Med*
1011 *Imaging Graph* 2005;29:235–41.
- 1012 46. Lee WB, Lee CD, Ho KI. A HIPAA-compliant key management scheme with
1013 revocation of authorization. *Comput Methods Prog Biomed* 2014;113:809–14.
- 1014 47. Provencher W. Automatic quantitation of localized in vivo 1H spectra with
1015 LCMoel. *NMR Biomed* 2001;14:260–4.
- 1016
1017
1018
1019
1020
1021
1022
1023
1024
1025
1026
1027
1028
1029